Calibration of Antenna Array with Dual Channel Switched Receiver System

Devanand Palur Palanivelu
Sensor Data & Information Fusion (SDF)
Fraunhofer FKIE
Wachtberg, Germany
devanand.palur.palanivelu@fkie.fraunhofer.de

Marc Oispuu
Sensor Data & Information Fusion (SDF)
Fraunhofer FKIE
Wachtberg, Germany
marc.oispuu@fkie.fraunhofer.de

***Abstract*—A precise estimation of the Direction of Arrival (DOA) of a signal is the fundamental functional requirement of antenna technology. A switched receiver system results in substantial reduction in hardware components, measurement complexity and cost of the entire system. In this paper, three diverse calibration methods are investigated on an array antenna with a dual channel switched receiver system. The calibration matrices are generated from the real measurements and implemented on the simulated and the real measurements. Robustness and flexibility of the calibration methods are compared in this paper. A conventional beamformer technique is implemented to perform Direction Finding (DF) of the calibrated system.**

***Index Terms*—switched receiver system, antenna array, calibration, multichannel signal processing**

I. Introduction

Estimation of Direction of Arrival of a signal is the primary objective of a Direction Finding algorithm. Although there are various high quality DF methods available, these processes are sensitive to the errors involved in the complete system. These errors affect the amplitude and phase of the signal received by an array which results in poor DOA estimation. The errors in an array antenna and in a receiver system, can be classified into static and dynamic [2]. A static error is caused by electrical and mechanical manufacturing tolerances, whereas dynamic errors are highly dependent on temperature and operating conditions. Mutual coupling is another major issue, which leads to mismatches of phase and amplitude between the elements of an array.

Antennas should be calibrated in order to compensate the deviations caused in a system because calibrated antennas possess the lowest signal-to-noise ratio requirement [3]. Calibration can be classified into offline and online. Offline methods require sources with known direction of the incident signals, whereas online methods do not. Offline and online methods were implemented and investigated in [4]–[9].

The typical measurement setup of an array antenna requires an equal number of receiving channels and antenna elements. If an array consists of many elements, then providing every element with a dedicated channel leads to an enormous increase of cost, measurement complexity and overall size of the system. In [10]–[12], the concept of an array system with reduced number of receiving channels was implemented and experimentally verified. Consider a receiver which has two

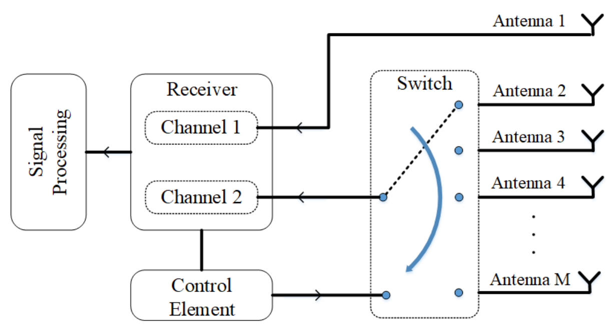

Fig. 1. Antenna array with dual channel switched receiver system

receiving channels where one element of an array is associated to the first channel and all other elements are connected to the second receiving channel by a switch as shown in Fig. 1. The acquired raw data are further processed to calibrate the system or to estimate the DOA of a signal.

This paper shows the adaptation of three different calibration processes, namely element pattern calibration, mutual coupling calibration and receiver phase calibration for an array antenna with a dual channel switched receiver system. The system is calibrated from the measurement data, which was acquired from a source with a known DOA. The chosen approaches are compared in terms of their performance and flexibility. Analysis revealed that element pattern calibration provided the best performance and mutual coupling method provided the highest flexibility.

This paper is organized as follows: Section II deals with the mathematical model of the investigated array antenna and the problems involved in calibration. Section III explains the preprocessing stage of a dual channel switched receiver system, creation and application of calibration methods. Section IV shows analysis of experimental results. Section V concludes the study.

In this article, $(\cdot)^*$ represents the conjugate complex, $(\cdot)^H$ represents the conjugate complex transpose. The notations .* and ./ denote element-wise multiplication and division, respectively.

978-9-0827-9703-9/19/$31.00 ©2019 IEEE

II. Array Model and Problem Formulation

An array of radius r with M elements is considered whose individual array elements are located at $\mathbf{r}_m$, $m = 1, ..., M$. The array is used to estimate the azimuth θ and elevation ϕ of a far-field source with a specific wavelength λ (Fig. 2).

The antenna array collects a batch of K data samples per measurement and the k-th data sample $\mathbf{y}_k \in \mathbb{C}^{M\times 1}$ reads

$$\mathbf{y}_k = \mathbf{a}(\theta, \phi)\, s_k + \mathbf{w}_k\,, \tag{1}$$

where s_k denotes the source signal and $\mathbf{w}_k$ indicates the receiver noise, $k = 1, ..., K$. The array steering vector

$$\mathbf{a}(\theta, \phi) = \operatorname{diag}[\mathbf{g}(\theta, \phi)]\ \mathbf{a}_0(\theta, \phi) \tag{2}$$

expresses the complex response of the antenna array with respect to a signal impinging from a direction (θ, ϕ). The mutual coupling phenomenon and dissimilarities in mechanical, electrical and directivity pattern between the elements constitute the non-ideal behaviour of the array elements, which is described by $\mathbf{g}(\theta, \phi)$. The m-th element of the ideal steering vector $\mathbf{a}_0(\theta, \phi)$ can be expressed as

$$a_{0,m}(\theta, \phi) = \exp\left(\mathrm{j}\tfrac{2\pi}{\lambda}\mathbf{e}^T(\theta, \phi)\,\mathbf{r}_m\right)\,, \tag{3}$$

where $\mathbf{e}(\theta, \phi)$ indicates the DOA unit vector.

In this paper, a dual channel switched receiver system is used to acquire the measurements (Fig. 1), i.e. the data from $M-1$ elements are measured in a switched format. The data samples of the dual channel switched receiver system are given by

$$\mathbf{z}_k = \mathbf{\Pi}_k\,\mathbf{y}_k\,, \tag{4}$$

where $\mathbf{\Pi}_k \in \{0, 1\}^{2\times M}$ denotes the switch matrix and it is constructed as

$$\mathbf{\Pi}_k = \begin{bmatrix} 1 & 0 & \cdots & 0 \\ 0 & \pi_{k,1} & \cdots & \pi_{k,M-1} \end{bmatrix} \tag{5}$$

with

$$\pi_{k,i} = \begin{cases} 1, & \text{if } iK' < k \leq (i+1)K' \\ 0, & \text{otherwise} \end{cases}$$

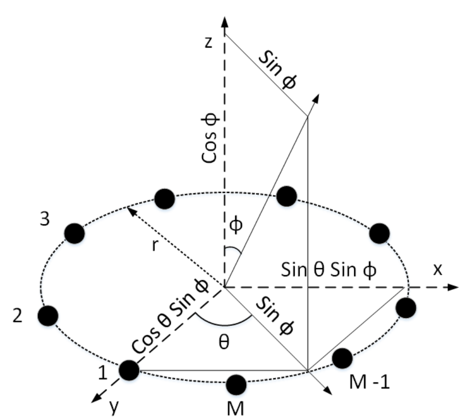

Fig. 2. Element positions of a UCA

for the i-th switch interval, $i = 1, ..., M-1$ [13]. This way, $K' = \frac{K}{M-1}$ samples are collected per channel for each switch interval. All measurements can be comprised in the matrix $\mathbf{Z} = [\mathbf{z}_1 \cdots \mathbf{z}_K] \in \mathbb{C}^{2\times K}$, which can be expressed in the following form

$$\mathbf{Z} = \begin{bmatrix} \mathbf{z}_{1,1} & \cdots & \mathbf{z}_{1,M-1} \\ \mathbf{z}_{2,1} & \cdots & \mathbf{z}_{2,M-1} \end{bmatrix}\,, \tag{6}$$

where $\mathbf{z}_{p,i}$ contains K' samples measured from the p-th channel during the i-th switch interval, $p = 1, 2$, $i = 1, ..., M-1$.

In order to determine the non-ideal behaviour of the system given by $\mathbf{g}(\theta, \phi)$, R measurements with a known DOA (θ_r, ϕ_r) are performed, which are denoted by $\mathbf{Z}_r$, $r = 1, ..., R$.

Then, the calibration problem can be stated as follows: Calculate a calibration term that considers the non-ideal behaviour of the system based on the measurement set $\mathbf{Z}_r$, $r = 1, ..., R$ of the dual channel switched receiver system. The receiver noise in the measurement is assumed to be an Additive White Gaussian Noise (AWGN) with zero mean and definite standard deviation which is spatially and temporally uncorellated.

III. Calibration Methods

A. Data Preprocessing

In this section, preprocessing of the measurement $\mathbf{Z}$, generation and implementation of the various calibration methods are explained in detail. The amplitude and the phase differences between the channels are more significant than the absolute amplitude and phase of each channel [14]. Therefore the relative phase and amplitude of Channel 2 are calculated by normalizing it with respect to Channel 1. The normalization of (6) leads to

$$\tilde{\mathbf{Z}} = \begin{bmatrix} 1 & \cdots & 1 \\ \mathbf{z}_{2,1}./\mathbf{z}_{1,1} & \cdots & \mathbf{z}_{2,M-1}./\mathbf{z}_{1,M-1} \end{bmatrix}. \tag{7}$$

On rearranging (7) based on antenna elements, we get

$$\tilde{\tilde{\mathbf{Z}}} = \begin{bmatrix} 1 \\ \tilde{\tilde{\mathbf{z}}}_2 \\ \vdots \\ \tilde{\tilde{\mathbf{z}}}_M \end{bmatrix} = \begin{bmatrix} 1 \\ \mathbf{z}_{2,1}./\mathbf{z}_{1,1} \\ \vdots \\ \mathbf{z}_{2,M-1}./\mathbf{z}_{1,M-1} \end{bmatrix} \tag{8}$$

with $\tilde{\tilde{\mathbf{z}}}_m = (b_{m,1}\,\mathrm{e}^{\mathrm{j}\varphi_{m,1}}, \ldots, b_{m,K'}\,\mathrm{e}^{\mathrm{j}\varphi_{m,K'}})^T$. The mean measurement vector $\bar{\mathbf{z}} = (\bar{b}_1\,\mathrm{e}^{\mathrm{j}\bar{\varphi}_1}, ..., \bar{b}_M\,\mathrm{e}^{\mathrm{j}\bar{\varphi}_M})^T$ can be calculated by

$$\bar{b}_m = \frac{1}{K'}\sum_{k=1}^{K'} b_{m,k}\,,$$

$$\bar{\varphi}_m = \arctan\left(\sum_{k=1}^{K'}\sin(\varphi_{m,k}), \sum_{k=1}^{K'}\cos(\varphi_{m,k})\right).$$

For R reference DOAs the full measurement set is

$$\bar{\mathbf{Z}} = [\bar{\mathbf{z}}_1 \cdots \bar{\mathbf{z}}_R]\,.$$

This measurement set corresponds to the following set of ideal array steering vectors (3)

$$\mathbf{A}_0 = [\mathbf{a}_0(\theta_1, \phi_1) \cdots \mathbf{a}_0(\theta_R, \phi_R)]\,.$$

B. Determination of Array Calibration

Calibration is performed to diminish the anomalies in a system and to estimate a plausible DOA with a higher level of precision. It is achieved by comparing the measurement $\bar{\mathbf{Z}}$ with a theoretical model $\mathbf{A}_0$. In this section, three diverse systematic calibration approaches are explained which are based on an assumption that,

$$\bar{\mathbf{Z}} \approx \mathbf{C}(\theta, \phi)\mathbf{A}_0, \tag{9}$$

where $\mathbf{C}(\theta, \phi)$ represents in general a calibration matrix. The proposed methods are classified based on the directional dependency of its application. The calibration methods are ordered in a decreasing order of complexity and quality:

1. Element pattern calibration,
2. Mutual coupling calibration and
3. Receiver phase calibration.

1) Element pattern calibration: This method identifies the phase difference between the actual measurement $\bar{\mathbf{Z}}$ and the ideal array steering matrix $\mathbf{A}_0$ and it is dependent on the direction of the signal. Let us consider

$$\boldsymbol{\Delta} = \bar{\mathbf{Z}} .* \mathbf{A}_0^* = [\boldsymbol{\Delta}(\theta_1, \phi_1) \cdots \boldsymbol{\Delta}(\theta_R, \phi_R)] \tag{10}$$

that contains the element pattern for all considered reference measurements. Then, the calibration matrix for a specific DOA (θ, ϕ) can be calculated by performing an interpolation of the corresponding element patterns $\boldsymbol{\Delta}(\theta_r, \phi_r)$, $r = 1, ..., R$

$$\mathbf{C}_1(\theta, \phi) = \mathrm{diag}\left[\boldsymbol{\Delta}(\theta, \phi)\right]. \tag{11}$$

The quality of the calibration matrix is directly proportional to the number of measurements R. It is evident that the array calibration is more precise for the considered reference DOAs. If the specific DOA to be estimated lies between or outside the region of the calibrated DOAs, then the required calibration vector $\boldsymbol{\Delta}(\theta, \phi)$ is interpolated from $\boldsymbol{\Delta}$.

2) Mutual coupling calibration: Mutual coupling is an inevitable phenomenon of an array, which is due to coupling of signals between elements in transmission and in reception modes. Minimizing the mutual coupling error along with gain-phase distortions can be accomplished by considering the actual measurement for calibration.

$$\mathbf{C}_2 = \bar{\mathbf{Z}}\mathbf{A}_0^H(\mathbf{A}_0\mathbf{A}_0^H)^{-1} \tag{12}$$

The calibration matrix is generated by taking R measurements into account. $\mathbf{C}_2$ can be applied to the DOAs which were not used to calculate it.

3) Receiver phase calibration: This approach is formed in order to compensate the existing phase distortion. Let $\boldsymbol{\Delta}_{m,r}$ denotes an element of (10), which is a complex number with definite amplitude $|\boldsymbol{\Delta}_{m,r}|$ and phase $\alpha_{m,r}$.

$$\delta_m = \frac{1}{R}\sum_{r=1}^{R} |\boldsymbol{\Delta}_{m,r}|$$

for $m = 1, ..., M$, $\boldsymbol{\delta} = (\delta_1, \delta_2, \ldots, \delta_M)^T$.

$$\bar{\alpha}_m = \arctan\left(\sum_{r=1}^{R}\sin(\alpha_{m,r}), \sum_{r=1}^{R}\cos(\alpha_{m,r})\right)$$

for $m = 1, ..., M$, $\bar{\boldsymbol{\alpha}} = (\mathrm{e}^{\mathrm{j}\alpha_1}, \mathrm{e}^{\mathrm{j}\alpha_2}, \ldots, \mathrm{e}^{\mathrm{j}\alpha_M})^T$. The receiver phase calibration matrix is calculated by

$$\mathbf{C}_3 = \mathrm{diag}(\boldsymbol{\delta} .* \bar{\boldsymbol{\alpha}}) \tag{13}$$

Like the mutual coupling method, the receiver phase calibration method can be applied to all DOAs. However this approach corrects only the phase imperfections but not the erros induced in the measurement due to mutual coupling effect.

When $R = 1$, the receiver phase calibration is executed based on single DOA and it is denoted by $\mathbf{C}_4$. This indicates the low quality and low complexity of the method. Though the array is calibrated only for one DOA, it is implemented for the complete array. Despite of its low complexity, this method does not demand extensive measurements which in turn reduces the measurement time and difficulty in creating a measurement setup. Often a measurement at $\phi_1 = 0°$ is used to measure a planar array to perfectly calibrate the sensor in zenith direction.

C. Application of Array Calibration

Let $\mathbf{C}$ denote a calibration matrix in a generic manner. Consider a measurement $\mathbf{z}_k$ given by (4), the calibration matrices can be applied as follows (refer (9)).

$$\mathbf{a}_{\mathrm{cal}}(\theta, \phi) = \mathbf{C}\,\mathbf{a}_0(\theta, \phi), \tag{14}$$

where $\mathbf{a}_{\mathrm{cal}}(\theta, \phi)$ indicates the calibrated array steering vector for a signal with specific DOA (θ, ϕ) and $\mathbf{a}_{\mathrm{cal}}(\theta, \phi)$ is further processed to estimate the DOA. The proposed calibration methods are applicable for azimuth θ and elevation ϕ estimation.

The covariance matrix $\mathbf{R}$ of the measurement $\mathbf{Z}$ collected by an array of M elements is calculated as

$$\mathbf{R} = \frac{1}{K}\sum_{k=1}^{K}\mathbf{z}_k\mathbf{z}_k^H .$$

As an example, a conventional BF algorithm was implemented to perform DF because it is optimal for the estimation of a single source.

$$(\hat{\theta}, \hat{\phi})_{\mathrm{BF}} = \arg\max_{\theta,\phi} \frac{\mathbf{a}_{\mathrm{cal}}^H(\theta, \phi)\ \mathbf{R}\ \mathbf{a}_{\mathrm{cal}}(\theta, \phi)}{\mathbf{a}_{\mathrm{cal}}^H(\theta, \phi)\ \mathbf{a}_{\mathrm{cal}}(\theta, \phi)}. \tag{15}$$

The generated calibration matrices can be applied to other DF algorithms.

IV. Experimental Results

A robust and compact Uniform Circular Array (UCA) with $M = 9$ omni-directional antenna elements along with a dual channel switched receiver system are designed to estimate the DOA of a signal for Unmanned Ground Vehicle (UGV) application. Especically in a scenario where the sensor platform and source are mobile, the accuracy of the DOA estimation is a critical aspect. Therefore an extensive set of measurements will be immensely beneficial to calibrate the array as precisely as possible. The UCA was mounted on a controllable rotating platform and a narrowband signal is measured. Therefore measurements were performed for every 1° of angular displacement which provides an intensive data set with $R = 360$ measurements. In this paper, only the azimuth θ is considered as a parameter of estimation. Therefore the signals were measured by positioning the transmitting antenna and the UCA at the same altitude, with constant elevation $\phi = 90°$. Thereby we eliminate ϕ as a parameter in the calibration and in the DF stage. For a closely packed antenna elements and a signal arriving from a far-field, the amplitude of the received signal does not possess useful directional information. Hence only the phase calibration is performed in the suggested methods. Although a UCA is used in this experiment to perform measurements, the calibration methods can be applied to different array geometries.

A. Algorithm Generation and Implementation

The algorithms shown in Fig. 3 are constructed with high modularity to generate and implement the calibration matrices. The quality and the complexity of a calibration matrix depend on the angular step size (S). For example, if the angular step size (S) equals 2°, then the total number of considered angular directions for the calibration equals $R = 180$. The created calibration matrices are tested in a simulated environment. The Signal-Noise-Ratio (SNR) and LOOP are the parameters to define the Monte-Carlo simulation, where LOOP denotes the number of times the DF process is executed for a particular angle (idx).

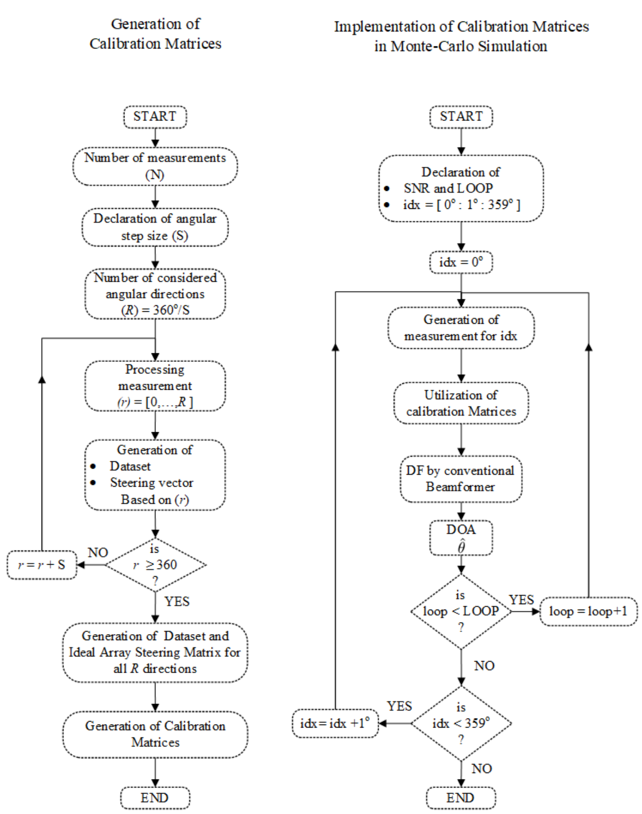

Fig. 3. Generation and implementation of the calibration methods

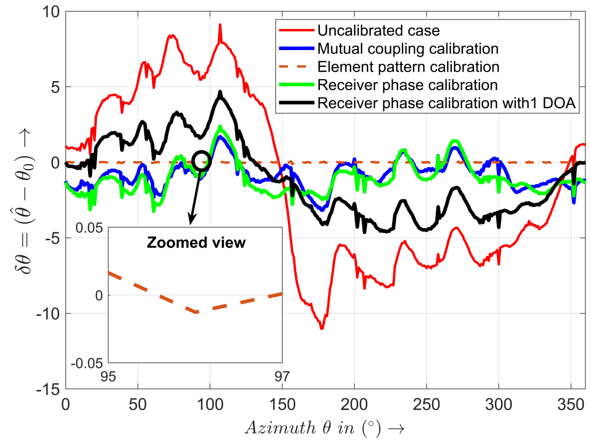

Fig. 4. Comparison of the calibration methods based on the DOA result

B. Simulation Result Analysis

Fig. 4 shows the distribution of the error $\delta\theta = (\hat{\theta} - \theta_0)$, where $\hat{\theta}$ and θ_0 represent the estimated DOA and ideal DOA, respectively. The calibration matrices were created by considering 360 measurements and their influence on the performance of the DOA estimation in a simulated scenario is shown in Fig. 4. It is clearly seen that the error is larger in an uncalibrated case than in all other calibrated cases. Among the calibration methods, receiver phase calibration method based on $R = 1$ DOA has the least complexity and it provides the worst compensation of the induced and existing errors in the UCA. In element pattern calibration, the transformation of the inherent steering vector for the calibrated angles yields the most accurate DOA estimation (in comparison to the other methods). Mutual coupling method has performed marginally better than receiver phase calibration method, because it did include the gain-phase distortion and the mutual coupling effect by considering the entire measurement.

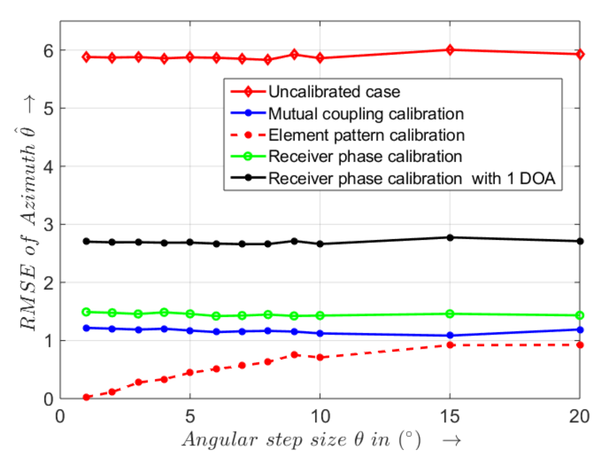

Fig. 5. Comparison of RMSE of $\hat{\theta}$ based on simulation

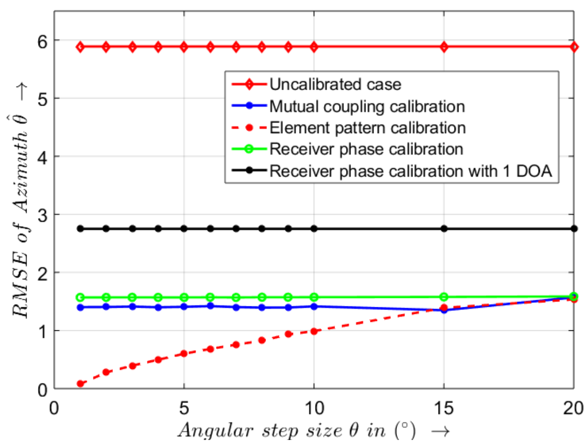

Fig. 6. Comparison of RMSE of $\hat{\theta}$ based on real measurement

Different angular step sizes provide different numbers of measurements available for the creation of calibration matrices (refer Section IV-A). These calibration matrices were tested in a simulated environment and the obtained results are displayed in Fig. 5. It is evident that the mutual coupling method, receiver phase calibration and receiver phase calibration based on 1 DOA possess a higher flexibilty by providing a similar RMSE of $\hat{\theta}$ for different step sizes. Element pattern calibration demonstrates a significant increase in RMSE of $\hat{\theta}$ with the growth of angular step size. This obviously elucidates that element pattern calibration method functions better only in the incident directions which were used to calibrate the UCA and the quality of element pattern calibration depends on R. Inspite of this behaviour, within the investigated angular step size, element pattern calibration has exhibited an enhanced behaviour in comparison to other calibration methods.

The created calibration matrices were implemented on the actual measurements which were used to generate the calibration matrices and the result is shown in Fig. 6. This approach reveals the versatility of the calibration methods. Through this analysis, it is proven that the mutual coupling method perfroms better compared to the receiver phase calibration approach and thus verifies the result shown in Fig. 5.

V. Conclusion

Calibration of a UCA with a dual channel switched receiver system is presented in this paper. The three selected calibration approaches are Element pattern calibration, mutual coupling calibration and receiver phase calibration. The calibration matrices are generated from a real measurement and they are tested on a simulated measurement to estimate the DOA. The presented analysis shows that with an angular step size of $1°$, the element pattern calibration delivers the best result. Mutual coupling method has performed marginally better than receiver phase calibration. Element pattern calibration has the least flexibilty within the tested angular step size region, while other methods yield a stable performance even with smaller number of measurements used to create calibration matrices. These calibration methods have been sucessfully tested on the measurement.

Acknowledgment

The authors would like to thank Sven Rau for his contributions to the work presented in this paper.

References

[1] H. Krim and M. Viberg, “Two decades of array signal processing research: the parametric approach,” *IEEE Signal Processing Magazine*, vol. 13, no. 4, pp. 67–94, July 1996.

[2] N. Tyler, B. Allen, and H. Aghvami, “Adaptive antennas: the calibration problem,” *IEEE Communications Magazine*, vol. 42, no. 12, pp. 114–122, Dec 2004.

[3] E. K. L. Hung, “Matrix-construction calibration method for antenna arrays,” *IEEE Transactions on Aerospace and Electronic Systems*, vol. 36, no. 3, pp. 819–828, July 2000.

[4] J. Pierre and M. Kaveh, “Experimental performance of calibration and direction-finding algorithms,” in *[Proceedings] ICASSP 91: 1991 International Conference on Acoustics, Speech, and Signal Processing*, April 1991, pp. 1365–1368 vol.2.

[5] M. Lin and L. Yang, “Blind calibration and doa estimation with uniform circular arrays in the presence of mutual coupling,” *IEEE Antennas and Wireless Propagation Letters*, vol. 5, pp. 315–318, 2006.

[6] Boon Chong Ng and Chong Meng Samson See, “Sensor-array calibration using a maximum-likelihood approach,” *IEEE Transactions on Antennas and Propagation*, vol. 44, no. 6, pp. 827–835, June 1996.

[7] M. Wang, X. Ma, S. Yan, and C. Hao, “An autocalibration algorithm for uniform circular array with unknown mutual coupling,” *IEEE Antennas and Wireless Propagation Letters*, vol. 15, pp. 12–15, 2016.

[8] W. Li, J. Lin, Y. Zhang, and Z. Chen, “Joint calibration algorithm for gain-phase and mutual coupling errors in uniform linear array,” *Chinese Journal of Aeronautics*, vol. 29, no. 4, pp. 1065 – 1073, 2016.

[9] H. Mir, J. Sahr, G. F. Hatke, and C. M. Keller, “Passive source localization using an airborne sensor array in the presence of manifold perturbations,” *Signal Processing, IEEE Transactions on*, vol. 55, pp. 2486 – 2496, 07 2007.

[10] J. Sheinvald and M. Wax, “Localization of multiple signals using subarrays data,” in *1995 International Conference on Acoustics, Speech, and Signal Processing*, vol. 3, May 1995, pp. 2112–2115 vol.3.

[11] W. Wu, C. C. Cooper, and N. A. Goodman, “Switched-element direction finding,” *IEEE Transactions on Aerospace and Electronic Systems*, vol. 45, no. 3, pp. 1209–1217, July 2009.

[12] J. Sheinvald and M. Wax, “Direction finding with fewer receivers via time-varying preprocessing,” *Signal Processing, IEEE Transactions on*, vol. 47, pp. 2 – 9, 02 1999.

[13] C. Steffes, C. Allmann, and M. Oispuu, “Fused single sensor emitter localization using time-multiplex aoa and s4tdoa measurements,” in *2018 Sensor Data Fusion: Trends, Solutions, Applications (SDF)*, Oct 2018, pp. 1–6.

[14] G. V. Tsoulos and M. A. Beach, “Calibration and linearity issues for an adaptive antenna system,” in *1997 IEEE 47th Vehicular Technology Conference. Technology in Motion*, vol. 3, May 1997, pp. 1597–1600 vol.3.